Bimetallic Silica-Supported Catalysts Based on Ni−Sn, Pd−Sn, and Pt−Sn as Materials in the CO Oxidation Reaction

J. Araña, P. Ramirez de la Piscina,* J. Llorca, J. Sales, and N. Homs*

Departament de Química Inorgànica, Facultat de Química, Universitat de Barcelona, Diagonal 647, 08028 Barcelona, Spain

J. L. G. Fierro

Instituto de Catálisis y Petroleoquímica, C.S.I.C., Cantoblanco, 28049 Madrid, Spain

Received November 6, 1997. Revised Manuscript Received February 23, 1998

Silica-supported bimetallic MSn (M = Ni, Pd, Pt) samples have been prepared by two consecutive impregnation steps with solutions of $[MCl_2(PPh_3)_2]$ complexes and $SnCl_2$, respectively. After treatment in H_2 at 673 K, these materials were characterized in detail by X-ray diffraction (XRD), conventional transmission electron microscopy, combined with energy-dispersive X-ray microanalysis, high-resolution transmission electron microscopy (HRTEM), and X-ray photoelectron spectroscopy (XPS). In addition, their performance in CO oxidation at temperatures ranging from 298 to 623 K was examined after activation processes under O_2 and/or CO/O_2 mixtures. XRD, HRTEM, electron diffraction, and XPS data of the Pt- or Pd-containing samples revealed that MSn alloys are formed upon H_2 treatment but that they are inactive in CO oxidation at low temperature. However, an oxidizing pretreatment produced alloys enriched in Pt or Pd (Pt_3Sn, Pd_3Sn_2) and SnO_x phases, which gave satisfactory catalytic performance in the CO oxidation. The behavior of the NiSn system was different. Although a Ni-enriched Ni_3Sn_2 phase was identified in reduced samples, further O_2 treatment at 673 K led to a mixture of phases including NiO and Ni-rich particles embedded in Sn-rich structures. This $NiSn/SiO_2$ sample gave poor performance in CO oxidation, which was similar to that of the Ni-free Sn/SiO_2 counterpart.

Introduction

Many works have been devoted to the study of CO oxidation reaction on SnO_2-supported Pt or Pd catalysts.[1−4] An area of particular interest is their application in closed-cycle operation of CO_2 lasers, where CO and O_2 at low concentrations are to be combined in mild conditions.[5,6] Their catalytic behavior is highly influenced by pretreatment conditions.[7−11] The possible formation of bimetallic phases during reductive pretreatments has been pointed out. However, authors do not always agree in their explanation of the contribution of the pretreatment conditions. Schryer et al. have shown that reductive pretreatment with H_2 or CO enhances the activity of Pt/SnO_x catalysts.[10,11] They propose that after reduction, metallic Pt and Sn formed are present predominantly as a PtSn alloy with some hydroxy groups, which are involved in CO oxidation, and they suggest a mechanism in which this alloy is involved, with Pt and Sn keeping the chemisorption properties in the PtSn alloy.[11] Other authors have found that H_2 pretreatment decreased CO_2 production; this has also been related to the formation of PtSn alloys.[8,9]

In this work we approached these systems from another point of view. Recently, we prepared well-defined silica-supported platinum−tin alloys.[12,13] Among them, PtSn alloy showed high performance in the catalytic activation of CO_2 and high selectivity for dehydrogenation reactions of hydrocarbons.

We used similar preparation methods to prepare bimetallic silica-supported catalysts from a group 10 metal and tin. The catalysts were characterized after reduction, and the presence of several supported bime-

* To whom all correspondence should be addressed.

(1) Bond, G. C.; Molloy, L. R.; Fuller, M. J. *J. Chem. Soc., Chem. Comm.* **1975,** 796.
(2) Gardner, S. D.; Hoflund, G. B.; Schryer, D. R.; Upchurch, B. T. *J. Phys. Chem.* **1991**, *95*, 835.
(3) Gangal, N. D.; Gupta, N. M.; Iyer, R. M. *J. Catal.* **1990**, *126*, 13.
(4) Sermon, P. A.; Self, V. A.; Barrett, E. P. S. *J. Mol. Catal.* **1991**, *65*, 377.
(5) Stark, D. S.; Harris, M. R. *J. Phys. E: Sci. Instrum.* **1983**, *16*, 492.
(6) Stark, D. S.; Crocker, A.; Steward, G. J. *J. Phys. E: Sci. Instrum.* **1983**, *16*, 158.
(7) Gardner, S. D.; Hoflund, G. B.; Davidson, M. R.; Schryer, D. R. *J. Catal.* **1989**, *115*, 132.
(8) Gadgil, M. M.; Sasikala, R.; Kulshreshtha, S. K. *J. Mol. Catal.* **1994**, *87*, 297.
(9) Tripathi, A. K.; Gupta, N. M. *J. Catal.* **1995**, *153*, 208.
(10) Schryer, D. R.; Upchurch, B. T.; Van Norman, J. D.; Brown, K. G.; Schryer, J. *J. Catal.* **1990**, *122*, 193.
(11) Schryer, D. R.; Upchurch, B. T.; Sidney, B. D.; Brown, K. G.; Hoflund, G. B.; Herz, R. K. *J. Catal.* **1991**, *130*, 314.
(12) Llorca, J.; Ramírez de la Piscina, P.; Fierro, J. L. G.; Sales, J.; Homs, N. *J. Catal.* **1995**, *156*, 139.
(13) Llorca, J.; Ramírez de la Piscina, P.; Fierro, J. L. G.; Sales, J.; Homs, N. *J. Mol. Catal. A* **1997**, *118*, 101.

S0897-4756(97)00728-X CCC: $15.00 © 1998 American Chemical Society
Published on Web 04/08/1998

Table 1. Chemical Analysis of Catalysts

catalyst	Ni, Pd, or Pt (wt %)	Sn (wt %)
$NiSn/SiO_2$	1.98	4.19
$PdSn/SiO_2$	2.51	2.68
$PtSn/SiO_2$	2.65	1.83
Sn/SiO_2		3.00

tallic alloys was determined. The goal of this work was to study the behavior of these bimetallic alloys in the CO oxidation reaction. Several processes for the activation of the materials were studied, and the catalysts were also characterized after these processes.

Experimental Section

Preparation of Catalysts. Silica-supported nickel−tin, palladium−tin, and platinum−tin catalysts were prepared following methods analogous to those reported for platinum−tin catalysts.[12]

The silica support was Aerosil Degussa (BET surface area of 200 $m^2\ g^{-1}$) partially dehydrated under high vacuum (10^{-6} Torr) at 473 K. First, each group 10 metal was impregnated separately from solutions of the $[MCl_2(PPh_3)_2]$ complexes, (acetone solution for $[NiCl_2(PPh_3)_2]$, tetrahydrofuran solution at 333 K for $[PdCl_2(PPh_3)_2]$, and methylene chloride solution for $[PtCl_2(PPh_3)_2]$), followed by a vacuum treatment (10^{-4} Torr) at 373 K overnight. In a second step, tin was impregnated from $SnCl_2$ acetone solution, and then samples were treated under high vacuum at 373 K overnight and reduced in flowing hydrogen at 673 K for 16 h. Catalysts were named: $NiSn/SiO_2$, $PdSn/SiO_2$, and $PtSn/SiO_2$. Catalysts were prepared with a theoretical metal content (Ni, Pd, or Pt) ca. 2−2.5% wt/wt and nominal atomic compositions NiSn, PdSn, and PtSn. As a reference catalyst, Sn/SiO_2 was prepared by impregnation of silica with an $SnCl_2$ acetone solution. The metallic content of catalysts determined by inductively coupled plasma (ICP) appears in Table 1.

Catalytic Activity. CO oxidation was carried out in a continuous-flow microreactor at atmospheric pressure. Catalysts (0.4−0.5 g) were rereduced in situ at 673 K for 1 h in flowing hydrogen, and then the behavior of catalysts in the CO oxidation reaction was studied. Several activation processes were tested, by treatments under flowing O_2 (20 $cm^3\ min^{-1}$) and/or $CO:O_2$ mixtures at temperatures from 423 to 673 K. The reaction was usually monitored from 623 K, as temperature was decreased until no CO_2 was produced or room temperature was reached. The catalytic activity at each temperature was determined after 2 h, when no changes in the activity were shown. When catalytic activity was studied at room temperature, the behavior was monitored for 12 h, and no change was observed during this time in any case. CO, CO_2, and O_2 were analyzed by on-line gas chromatography using a 3400 Varian GC equipped with an automated gas sample valve.

Catalyst Characterization. The XRD profiles were collected at a step width of 0.02° in the 2θ range of interest using a Siemens D-500 X-ray diffractometer equipped with a graphite monochromator and Cu target. Average size of particles was estimated by using the Scherrer formula at various high-intensity reflections corrected from Cu Kα2 radiation.

Conventional transmission electron microscopy (CTEM) combined with energy-dispersive X-ray microanalysis (EDX) was carried out with a Hitachi H 800-MT electron microscope working at 200 kV and equipped with a Kevex analytical system. EDX measurements were carried out in STEM mode. After EDX analysis, imaging of the area sampled revealed that a probe less than 5 nm was used in all cases.

High-resolution transmission electron microscopy (HRTEM) combined with EDX was performed using a Philips CM-30 electron microscope working at 300 kV equipped with a Link analytical system. Samples for analysis were suspended in methanol and placed on copper grids with a holey-carbon-film support.

Photoelectron spectra (XPS) were acquired with a VG Escalab 200R spectrometer equipped with a hemispherical electron analyzer and Mg Kα ($h\nu$ = 1253.6 eV) X-ray source. The powder samples were pressed into small stainless steel cylinders and then mounted on a heater placed in a pretreatment chamber. Prior to being moved into the analysis chamber the samples were treated for 2 h: the previously reduced samples treated in H_2 at 673 K, the previously oxidized samples in O_2 at 673 K. Some oxidized samples, after analysis, were moved back to the pretreatment chamber and exposed to $CO:O_2$ = 1:1 mixture for 2 h and then again analyzed. The residual pressure in the ion-pumped analysis chamber was maintained below 5×10^{-9} Torr during data acquisition. The intensities of Si 2p, Pt 4f, Pd $3d_{5/2}$, Ni $2p_{3/2}$, and Sn $3d_{5/2}$ peaks were estimated by calculating the integral of each peak after smoothing and subtraction of the "S-shaped" background and fitting the experimental curve by a least-squares routine supplied by the instrument manufacturer using Gaussian and Lorentzian lines. The binding energy (BE) reference was taken at the Si 2p peak from silica at 103.4 eV. An estimated error of ±0.1 eV can be assumed for all measurements.

Results

Catalytic Activity. Catalytic activity in the CO oxidation reaction was determined under several experimental conditions. After the rereduction of the catalyst in the reactor at 673 K, the first catalytic test was carried out. Then, before a new test, catalysts were activated under different experimental conditions in order to determine the suitable activation process for each catalyst. Once the activation conditions were determined, catalytic tests were carried out.

Reduced $PdSn/SiO_2$ catalyst was tested in the CO oxidation reaction with a reactant flow of a mixture of CO (16%) and O_2 (8%) diluted with N_2 (total flow 25 $cm^3\ min^{-1}$). Reduced $PdSn/SiO_2$ showed no activity under these conditions at 423 K. Then the $PdSn/SiO_2$ catalyst was treated under flowing pure oxygen (20 $cm^3\ min^{-1}$) for 1 h at increasing temperatures: 423, 473, 573, 648, and 673 K. After each oxidizing treatment, the $PdSn/SiO_2$ catalyst was tested in the CO oxidation reaction at 423 K under the experimental conditions specified above. In all cases, N_2 and CO were progressively introduced into the reactor and temperature was decreased, until the reference conditions at 423 K were reached. Only after a treatment under flowing oxygen at 673 K was the $PdSn/SiO_2$ active in the CO oxidation reaction at the reference conditions. Therefore, for this catalyst this pretreatment was considered the most suitable activation process, and it was applied before catalytic tests. Figure 1 displays results of some catalytic tests corresponding to $PdSn/SiO_2$. In all cases, the reaction temperature was lowered from 523 to 298 K, and conversion was determined after 2 h once the reaction temperature was reached. No changes in the conversion were observed after this time. The activity corresponding to 298 K was determined after 12 h of reaction at this temperature, and no changes in conversion were shown during this time. Then, to observe whether the catalyst behavior showed hysteresis cycle, after the experimental point at 298 K the catalytic test was repeated but now with temperatures increasing from 298 to 523 K. The same conversion values were obtained at each temperature.

One of the objectives of this work was to determine the influence of CO_2 concentration on the catalytic

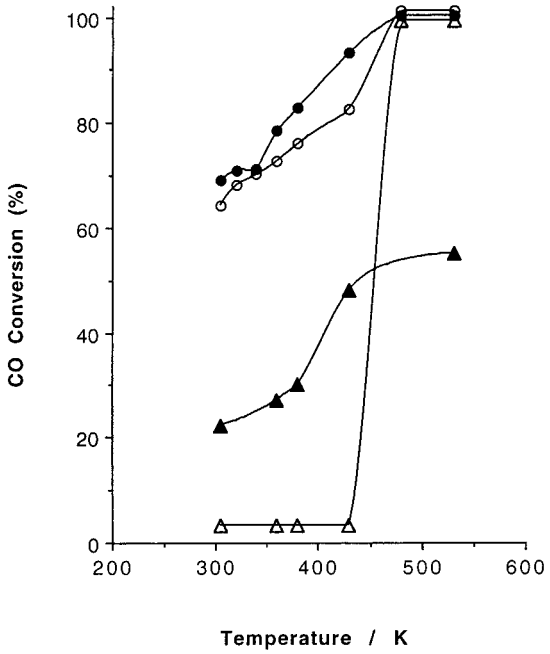

Figure 1. CO conversion for $PdSn/SiO_2$ catalyst in the CO oxidation reaction at atmospheric pressure, as a function of temperature, under different reactant flow conditions. Catalyst was pretreated under O_2 at 673 K. (○) N_2:CO:O_2, 19:4:2 cm^3 min^{-1}. (●) N_2:CO:O_2, 17:4:4 cm^3 min^{-1}. (▲) N_2:CO:O_2, 19:4:1 cm^3 min^{-1}. (△) N_2:CO:O_2 19:2:1 cm^3 min^{-1}.

Table 2. CO Conversion on the Catalytic Oxidation of CO over the $PdSn/SiO_2$ Catalyst as a Function of CO_2 Concentration in Reactant Gases

[CO_2] (%)	CO conversion (%)
0	63.0
8	62.2
16	62.7
28	62.9
40	62.5
48	62.6

[a] T = 298 K, P = 1 Atm. Reactant Flow (N_2 + CO + O_2 + CO_2) = 25 cm^3 min^{-1}, [CO] = 16%, [O_2] = 8%.

behavior of the materials under study. Thus, some experiments were carried out replacing N_2 by CO_2 at 298 K. Table 2 shows that, in the experimental conditions used, no change in the CO conversion was observed after replacing N_2 by CO_2 for the $PdSn/SiO_2$ catalyst.

A similar study of the effect of an oxidizing treatment on the behavior of $PtSn/SiO_2$ catalyst in the CO oxidation reaction was carried out. A pretreatment under oxygen at 673 K enhanced its catalytic behavior, and only after this treatment was the catalyst active below 398 K (Table 3). This activation process was also performed for this catalyst before carrying out the catalytic activity tests.

Results from catalytic tests corresponding to $PtSn/SiO_2$ are illustrated in Figure 2. Under the same experimental conditions, lower CO conversions were obtained when compared with those obtained with $PdSn/SiO_2$. Table 4 summarizes the effect of substitution of inert gas (Ar) by CO_2. A null effect is observed when high concentration of (CO:O_2) mixture in the reactant gases is used, but a high effect can be noted at lower (CO:O_2) concentrations. It is noteworthy that under the same experimental conditions no effect on CO conversion was observed for $PdSn/SiO_2$ catalyst.

Table 3. Effect of the Temperature of O_2 Treatment for the $PtSn/SiO_2$ Catalyst on the CO Conversion as a Function of Reaction Temperature[a]

	CO conversion (%)						
	O_2 treatment T (K)						
reaction T (K)	*b*	423	473	523	573	623	673
423	4	6	4	5	7	11	100
398	1	1	1	1	2	2	99
373	0	0	0	0	0	0	99
348	0	0	0	0	0	0	98
323	0	0	0	0	0	0	96

[a] Reaction conditions: total flow 26 cm^3 min^{-1}, N_2:CO:O_2 = 10:1:2, P = 1 Atm. [b] No O_2 treatment was carried out.

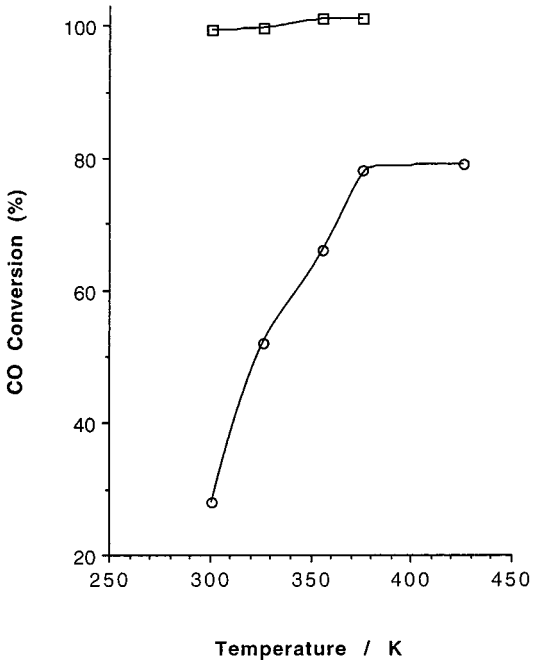

Figure 2. CO conversion for $PtSn/SiO_2$ catalyst in the CO oxidation reaction at atmospheric pressure, as a function of temperature, under different reactant flow conditions. Catalyst was pretreated under O_2 at 673 K. (○) Ar:CO:O_2, 19:4:2 cm^3 min^{-1}. (□) Ar:CO:O_2, 13:8:4 cm^3 min^{-1}.

Table 4. Effect of CO_2 Concentration in the Reactant Mixture upon CO Conversion for $PtSn/SiO_2$ Catalyst[a]

composition of reactant mixture			
[CO] (%)	[O_2] (%)	[CO_2] (%)	CO conversion (%)
16	8	0	27
16	8	32	0
24	12	0	100
24	12	8	100
24	12	32	100

[a] Reaction Conditions: T = 298 K, P = 1 Atm, Total Flow of Reactants (Ar + CO + O_2 + CO_2) = 25 cm^3 min^{-1}.

For comparison, an experiment was done with the Sn/SiO_2 catalyst. Reduced catalyst was pretreated under oxygen at 673 K, and then different catalytic tests were carried out (Table 5). Only at high temperatures or high O_2/CO ratios was the Sn/SiO_2 active. Under milder conditions in which $PdSn/SiO_2$ or $PtSn/SiO_2$ catalysts were active, Sn/SiO_2 was not.

$NiSn/SiO_2$ system either freshly reduced or after treatments under flowing O_2 up to 673 K gave poor catalysts, which needed much higher O_2/CO ratios and temperatures than $PtSn/SiO_2$ or $PdSn/SiO_2$ catalysts to give similar conversion levels. The activity data after

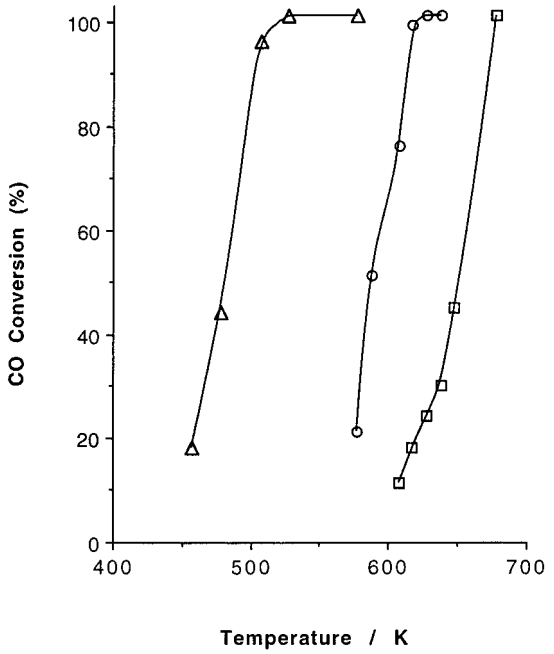

Figure 3. CO conversion for $NiSn/SiO_2$ catalyst in the CO oxidation reaction, at atmospheric pressure, as a function of temperature, under different reactant flow conditions. Catalyst was pretreated under O_2 at 673 K. (□) N_2:CO:O_2, 18:4:4 cm^3 min^{-1}. (○) N_2:CO:O_2, 22:2:2 cm^3 min^{-1}. (△) N_2:CO:O_2, 24:1:1 cm^3 min^{-1}.

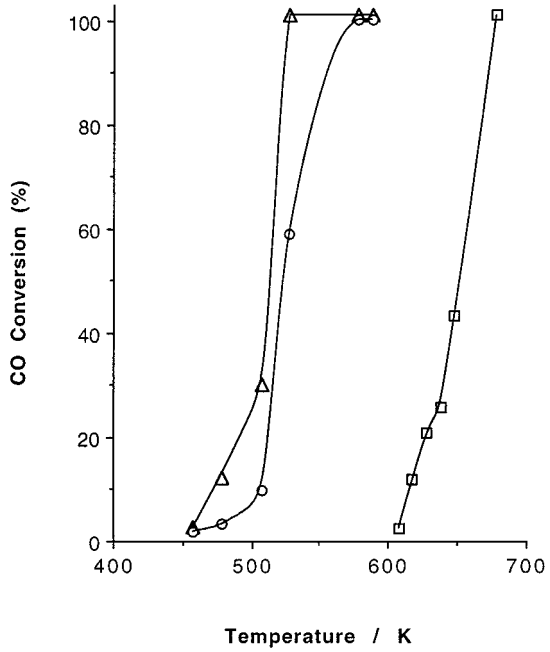

Figure 4. CO conversion for $NiSn/SiO_2$ catalyst in the CO oxidation reaction at atmospheric pressure, as a function of temperature, under different reaction conditions. Catalyst was pretreated under CO/O_2 at 673 K. (□) N_2:CO:O_2, 19:4:2 cm^3 min^{-1}. (○) N_2:CO:O_2, 10:2:1 cm^3 min^{-1}. (△) N_2:CO:O_2, 10:1:0.5 cm^3 min^{-1}.

Table 5. CO Conversion in the Catalytic Oxidation of CO at Atmospheric Pressure for Sn/SiO_2 Catalyst as a Function of Reaction Temperature, Reactant Flow, and Composition of Reactant Mixture

composition of reactant mixture					
flow (cm^3 min^{-1})	[CO] (%)	[O_2] (%)	[CO_2] (%)	T (K)	CO conversion(%)
20	10	90	0	623	100
20	20	80	0	573	100
25	16	8	0	473	0
25	32	16	0	523	100
25	32	16	0	473	28
25	32	16	8	473	0
22	9	91	0	473	100
22	9	91	0	298	100
12	17	83	0	298	0

an O_2 pretreatment at 673 K are presented in Figure 3. It can be seen that this catalyst showed a high variation in CO conversion for a narrow temperature interval. However, after a treatment under $CO:O_2$ (1:1) at 673 K this catalyst showed a different behavior, reaching higher conversion values even with stoichiometric $CO:O_2$ ratios (Figure 4). When the Sn/SiO_2 catalyst was used after a similar pretreatment, under the same experimental conditions, similar conversion values were obtained.

Catalyst Characterization. Catalysts were characterized by X-ray diffraction (XRD), TEM, electron diffraction (ED), EDX, and XPS techniques after both the reduction step and the activation process in order to determine the changes that influenced the behavior of the catalysts in the CO oxidation.

A complete characterization of $PtSn/SiO_2$ catalyst after the reduction step had been already carried out. The presence of only PtSn alloy supported on silica had been determined (particle size determined by TEM 24 × 8 nm).[12] As stated above, the most suitable activation process determined for this catalyst was a treatment at 673 K under flowing O_2 for 1 h, so the characterization of this catalyst after this treatment was accomplished.

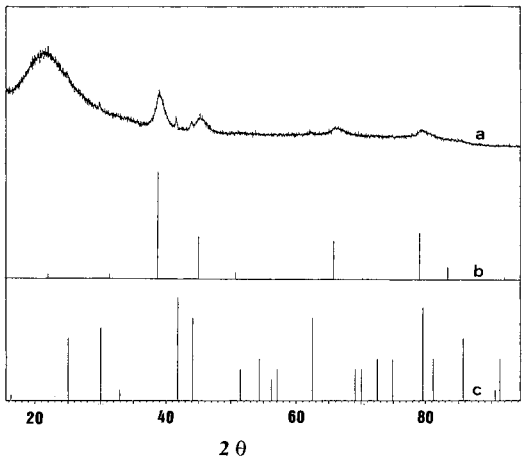

Figure 5. (a) XRD pattern of the $PtSn/SiO_2$ sample after O_2 treatment at 673 K. (b) XRD pattern of Pt_3Sn alloy. (c) XRD pattern of PtSn alloy.

Figure 5 shows the XRD pattern obtained after the oxidizing pretreatment; this technique showed an almost full transformation of the PtSn alloy present after the reduction to the Pt_3Sn alloy. New reflections appearing at $2\theta = 39°$, $2\theta = 45.5°$, $2\theta = 66°$ and $2\theta = 79.5°$ are characteristic of this cubic phase; small peaks corresponding to the presence of PtSn phase can be yet observed in the X-ray diffraction pattern at $2\theta = 41.5°$ and $2\theta = 44°$. The size of Pt_3Sn particles determined by this technique was 6.2 nm.

Bright- and dark-field transmission electron micrographs of $PtSn/SiO_2$ catalyst after the activation process are shown in Figure 6. The presence of isolated,

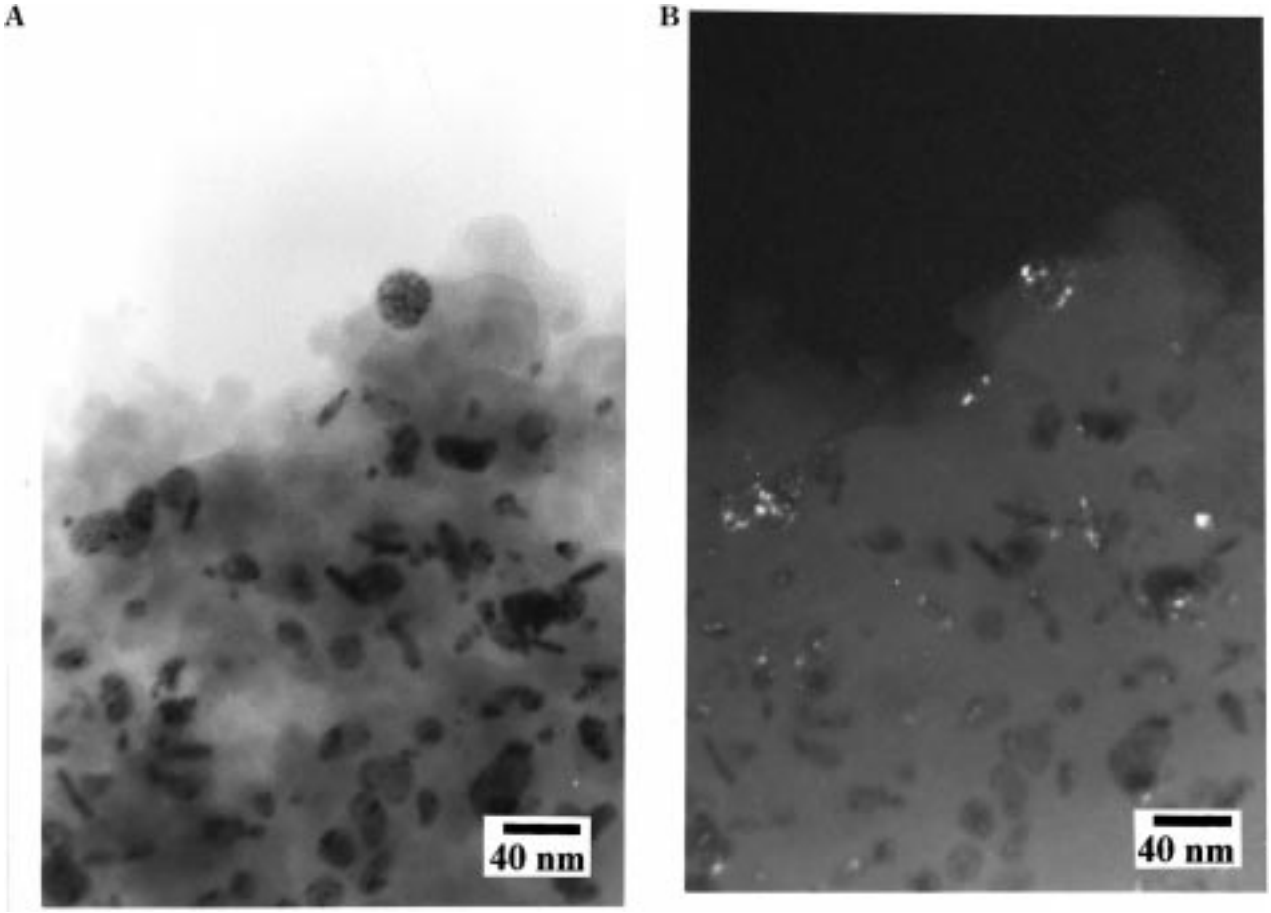

Figure 6. Bright-field (A) and dark-field (B) conventional transmission electron micrographs of the $PtSn/SiO_2$ sample after O_2 treatment at 673 K.

homogeneously distributed particles with an average size similar to that of the reduced catalyst is seen in the bright-field image (Figure 6A). These particles in turn contain multiple crystallites with different orientations as revealed in the dark-field mode (Figure 6B). A deeper analysis of particles by high-resolution electron microscopy indicated the presence of Pt_3Sn particles surrounded by an apron; the analysis by EDX of this layer showed that it was tin-rich. In Figure 7 two individual crystallites (indicated by arrows) of Pt_3Sn phase oriented in the [110] direction (lattice spacing 2.8 Å) can be seen. The selected-area electron diffraction pattern of this catalyst displays only the main reflections for Pt_3Sn alloy (inset Figure 7).

Surface characterization of $PtSn/SiO_2$ catalyst by XPS is summarized in Table 6; atomic ratios on the surface were calculated from XP spectra and sensitivity factors.[14] The estimated error of these measurements was below 10% in all cases. A treatment under flowing O_2 at 673 K for 2 h produced a partial oxidation of surface Pt^0 to Pt^{2+} (39%) species. In addition, a decrease in the concentration of platinum in the surface region was produced. The Pt/Sn surface atomic ratio after the oxidation process was 0.23, significantly lower than 1.10 found after the reduction process.[12] For this catalyst, XP spectra corresponding to Sn $3d_{5/2}$ level were resolved into three components. Even if tin was oxidized to a large extent, there was also evidence of alloyed tin and metallic tin.

(14) Wagner, C. D.; Davis, L. E.; Zeller, M. V.; Taylor, J. A.; Raymond, R. H.; Gale, L. H. *Surf. Interface Anal.* **1981**, *3*, 211.

A subsequent treatment under $CO:O_2$ mixture at 573 K decreased the Pt/Sn atomic ratio even further, and after this treatment the platinum in the surface region was markedly decreased whereas 21% of surface tin was still present as alloyed tin.

The most suitable activation process determined for $PdSn/SiO_2$ catalyst was also an oxidizing treatment under flowing O_2 at 673 K for 1 h. So, this catalyst was characterized after reduction and after the oxidizing treatment in order to show its transformation during the activation process, which improves its catalytic behavior in the CO oxidation reaction.

Figure 8 presents the XRD pattern corresponding to $PdSn/SiO_2$ catalyst after the reduction step and after the oxidizing pretreatment. After the reduction step (pattern a), all the diffraction peaks in the pattern of the catalyst correspond to the PdSn phase; however, this phase shows two reflections at $2\theta = 39.6°$ and $2\theta = 40.8°$, located at the same position as the two more intense peaks of the Pd_3Sn_2 alloy. So the presence of the Pd_3Sn_2 phase in the reduced catalyst cannot be ruled out completely. After the O_2 treatment at 673 K, the XRD pattern changed significantly. Now, the intensity of the reflections assigned to the PdSn alloy diminished except those located at $2\theta = 39.6°$ and $2\theta = 40.8°$. Besides, the appearance of reflections at $2\theta = 58.2°$ and $2\theta = 73.6°$, characteristic of the Pd_3Sn_2 phase that cannot be assigned to the PdSn phase, indicates the presence of silica-supported Pd_3Sn_2 after the oxidizing treatment. The presence of a SnO_2 phase may also be

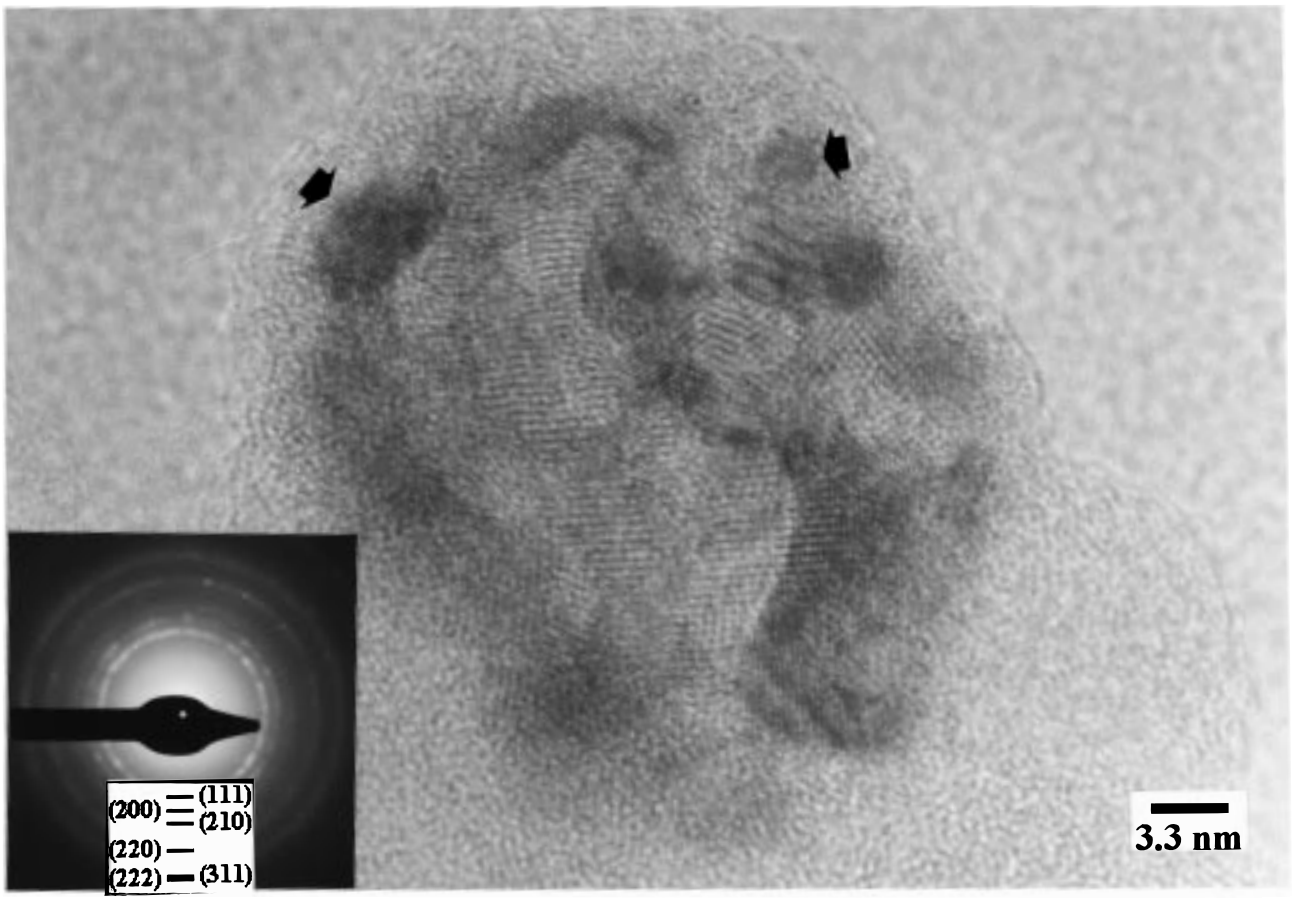

Figure 7. High-resolution electron microscopy image of a representative particle of the $PtSn/SiO_2$ sample after O_2 treatment at 673 K. Selected-area electron diffraction pattern (inset) shows the main reflections only for the Pt_3Sn alloy.

Table 6. Binding Energies (eV) of Core Electrons and XPS Atomic Ratios for $PtSn/SiO_2$ Catalyst after Different Treatment Conditions[a]

treatment	O 1s	Pt $4f_{7/2}$[b]	Sn $3d_{5/2}$[b]	Pt/Si	Sn/Si	Pt/Sn
O_2, $T = 673$ K	533.0	71.4(61) 72.5(39)	484.0(6) 485.4(11) 487.6(83)	0.0048	0.0210	0.228
CO/O_2, $T = 573$ K (previously O_2 at 673 K)	532.9	71.2	485.5(21) 487.3(79)	0.0005	0.0275	0.018

[a] A value of 103.4 eV was obtained for the Si 2p peak in all experiments. [b] Values in parentheses indicate the relative percentage of surface species for each sample.

proposed from the XRD pattern (reflections at $2\theta = 26.7°$ and $2\theta = 33.8°$).

Transmission electron microscopy of $PdSn/SiO_2$ after the reduction step showed a bimodal distribution of particle sizes: 25−60 and 200−300 nm. Their individual bimetallic nature can be inferred by EDX. Some of these particles were analyzed by high-resolution electron microscopy and electron diffraction, and it was possible in some cases to assign the pattern to the PdSn phase. This was accomplished with some particles of both sizes, 25−60 nm and 200−300 nm. Figure 9 shows the high-resolution electron microscopy image corresponding to one of these rhombic PdSn alloy particles, oriented in the [010] direction; in the figure are indicated the lattice spacings corresponding to (001) and (100) planes (6.3 and 6.1 Å, respectively). Figure 9 also shows the convergent-beam electron diffraction pattern corresponding to a particle of the PdSn phase oriented in the [010] direction. An inspection of Figure 9 also indicates that the particle was partly covered by a crystalline-poor layer (upper left), which was shown by EDX to be tin-rich.

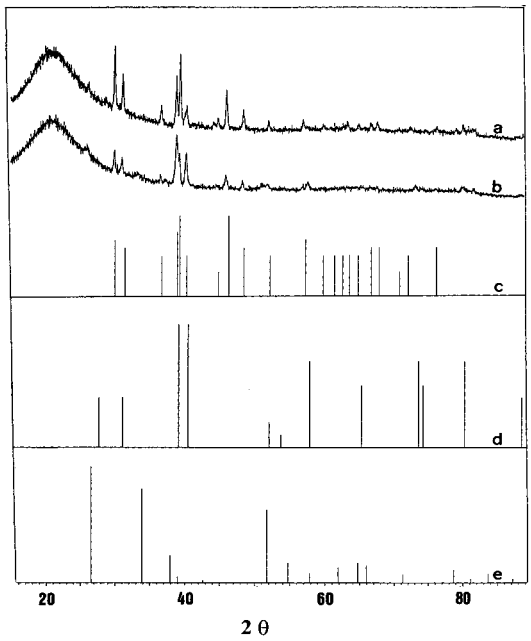

Figure 8. XRD pattern of the $PdSn/SiO_2$ catalyst (a) after H_2 treatment at 673 K and after (b) subsequent O_2 treatment at 673 K. (c) XRD pattern of PdSn alloy. (d) XRD pattern of Pd_3Sn_2 alloy. (e) XRD pattern of SnO_2.

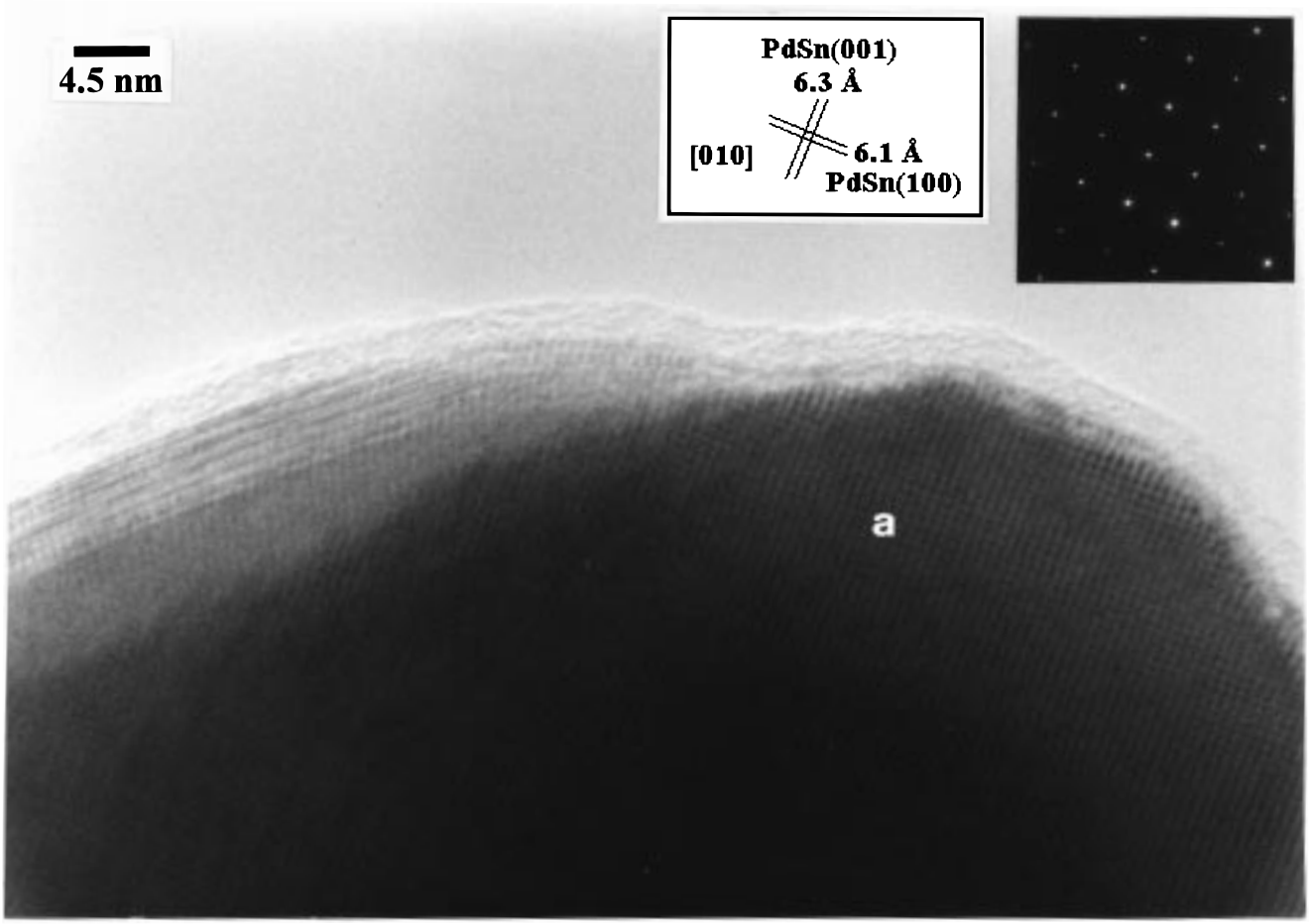

Figure 9. High-resolution electron microscopy image of a rhombic PdSn alloy particle in $PdSn/SiO_2$ sample after H_2 treatment at 673 K. Inset corresponds to lattice spacings and convergent-beam electron diffraction pattern obtained from area labeled "a".

Table 7. Binding Energies (eV) of Core Electrons and XPS Atomic Ratios for $PdSn/SiO_2$ Catalyst after Different Treatment Conditions[a]

treatment	Pd $3d_{5/2}$	Sn $3d_{5/2}$[b]	Pd/Si	Sn/Si	Pd/Sn
H_2, $T = 673$ K	336.2	484.9 (30) 486.5 (61) 487.7 (9)	0.0014	0.0372	0.037
O_2, $T = 673$ K	336.2	484.9 (30) 487.1 (70)	0.0005	0.0253	0.019
CO/O_2, $T = 673$ K	336.6	485.0 (24) 487.2 (76)	0.0005	0.0192	0.026

[a] A value of 103.4 eV was obtained for the Si 2p peak in all experiments. [b] Values in parentheses indicate the relative percentage of surface species for each sample.

Figure 10 shows a transmission electron micrograph of the catalyst $PdSn/SiO_2$ after pretreatment under flowing O_2 at 673 K for 1 h. Now a peripheral region covering the particles with a thickness of 6−8 nm is clearly seen (see area enclosed by arrows in Figure 10). EDX analysis showed that this region was tin-rich.

XP spectra corresponding to $PdSn/SiO_2$ catalyst after different treatments showed, in all cases, a poor Pd $3d_{5/2}$ signal due to a high Sn segregation on the suface. Table 7 compiles binding energies and surface atomic ratios for this catalyst. The Sn $3d_{5/2}$ peak for the $PdSn/SiO_2$ reduced catalyst shows three components. The component at lowest binding energy could be assigned to alloyed Sn (484.9−485.0 eV) and the other two components to oxidized species. Binding energies of the Sn $3d_{5/2}$ core level somewhat above 487 eV could be ascribed to tin oxide retaining chemisorbed oxygen. After O_2 treatment at 673 K, or subsequent $CO:O_2$ treatment, the Pd/Sn atomic ratio on the surface is even lower, but the ratio of alloyed Sn on the surface still remains around 30%.

The characterization of $NiSn/SiO_2$ catalyst was also carried out after different treatments. X-ray diffraction patterns corresponding to this catalyst are shown in Figure 11. After the reduction step, the XRD pattern can be assigned to the silica-supported nickel-enriched Ni_3Sn_2 alloy. When the catalyst was treated under oxygen at 673 K, a more complicated XRD pattern was obtained. In this pattern, the presence of Ni_3Sn_2 phase can still be observed, but crystalline phases of Ni_3Sn and SnO_2 can also be identified by this technique (the new peak appearing at $2\theta = 44.8°$ corresponds to the Ni_3Sn phase and peaks at $2\theta = 26.5°$, $2\theta = 33.8°$, and $2\theta = 51.8°$ correspond to SnO_2). After the oxidation treatment, a poor catalyst was obtained in the CO oxidation reaction, as stated above. Then, the catalyst was rereduced and pretreated under a $CO:O_2$ mixture before another set of catalytic tests were performed. The XRD pattern of this catalyst obtained after these experiments is also shown in Figure 11c. In this case, the presence of the Ni_3Sn_2 phase, now tin-enriched, is clearly revealed. $NiSn/SiO_2$ catalyst was observed by TEM after reduction and after O_2 treatment at 673 K. After reduction, big particles of 40−350 nm were observed, whose individual bimetallic nature was revealed by EDX. The electron diffraction pattern of some of these particles was obtained, and the cell parameters

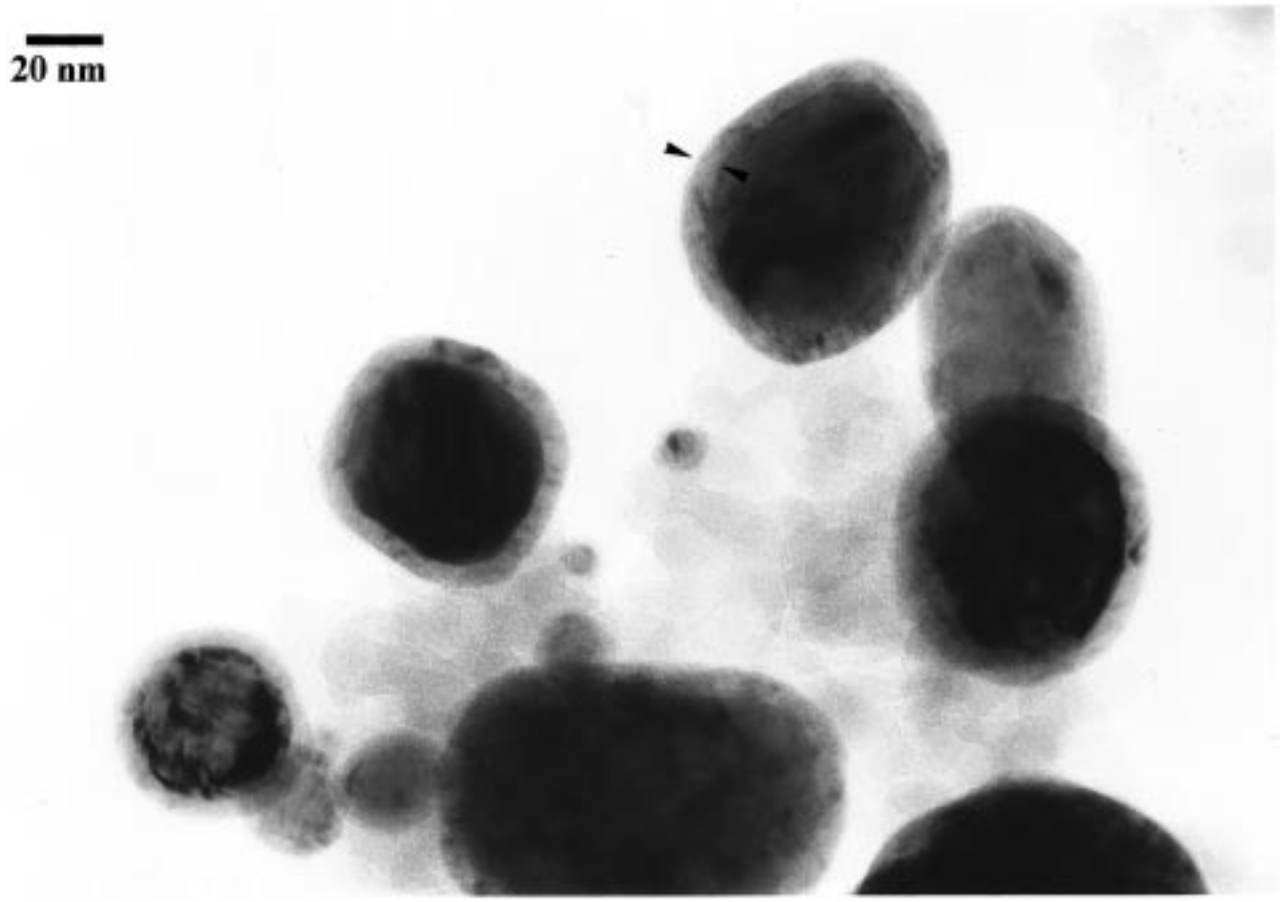

Figure 10. Transmission electron micrograph of the $PdSn/SiO_2$ sample after O_2 treatment at 673 K.

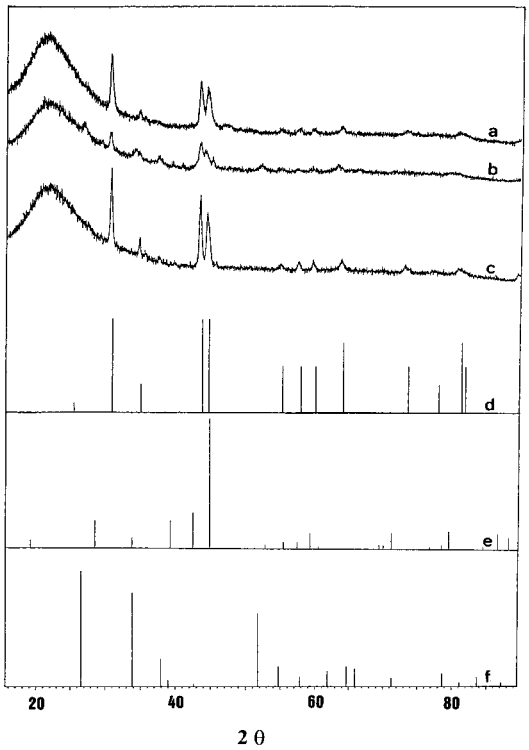

Figure 11. XRD pattern of the $NiSn/SiO_2$ catalyst (a) after H_2 treatment at 673 K and after (b) subsequent O_2 treatment at 673 K. (c) XRD pattern of the $NiSn/SiO_2$ catalyst after reaction. (d) XRD pattern of Ni_3Sn_2 alloy. (e) XRD pattern of Ni_3Sn alloy. (f) XRD pattern of SnO_2.

calculated from them agreed with those calculated from the XRD pattern for nickel-enriched Ni_3Sn_2 alloy.

Figure 12 shows a transmission electron micrograph corresponding to $NiSn/SiO_2$ catalyst after O_2 treatment at 673 K. The sample contained nickel-rich particles (see, for example, the particle marked by an arrow) embedded in tin-rich structures as shown by EDX analysis. Moreover, analysis by selected-area electron diffraction allowed identification of the NiO phase.

Table 8 shows XPS data for $NiSn/SiO_2$ after reduction or oxidation treatments. In both cases the Sn $3d_{5/2}$ peak can be resolved into three components, the component at ca. 484 eV can be assigned to reduced species (Sn^0), the peak around 486.0 eV to tin oxide, and the higher binding energy peak to tin oxide on which oxygen is chemisorbed. For the Ni $2p_{3/2}$ level, two components referred to as Ni^0 and Ni^{2+} species can be observed. Oxidation treatment produced a slight decrease in surface Sn or Ni species and in their reduced/oxidized ratios. In both cases, after reduction or O_2 treatment, high values of Ni/Sn surface ratio were found, which contrast with $PtSn/SiO_2$ and $PdSn/SiO_2$ catalysts.

Discussion

For the $PtSn/SiO_2$ catalyst, taking into account the characterization results from XRD and TEM experiments, it could be proposed that the main part of the PtSn bimetallic phase supported on silica present on the catalyst after the reduction step evolves, when treated with O_2 at 673 K, to a Pt_3Sn phase surrounded by tin oxide. However XPS analysis showed that after the activation process a small percentage of tin still remained as alloyed tin on the surface region. Although

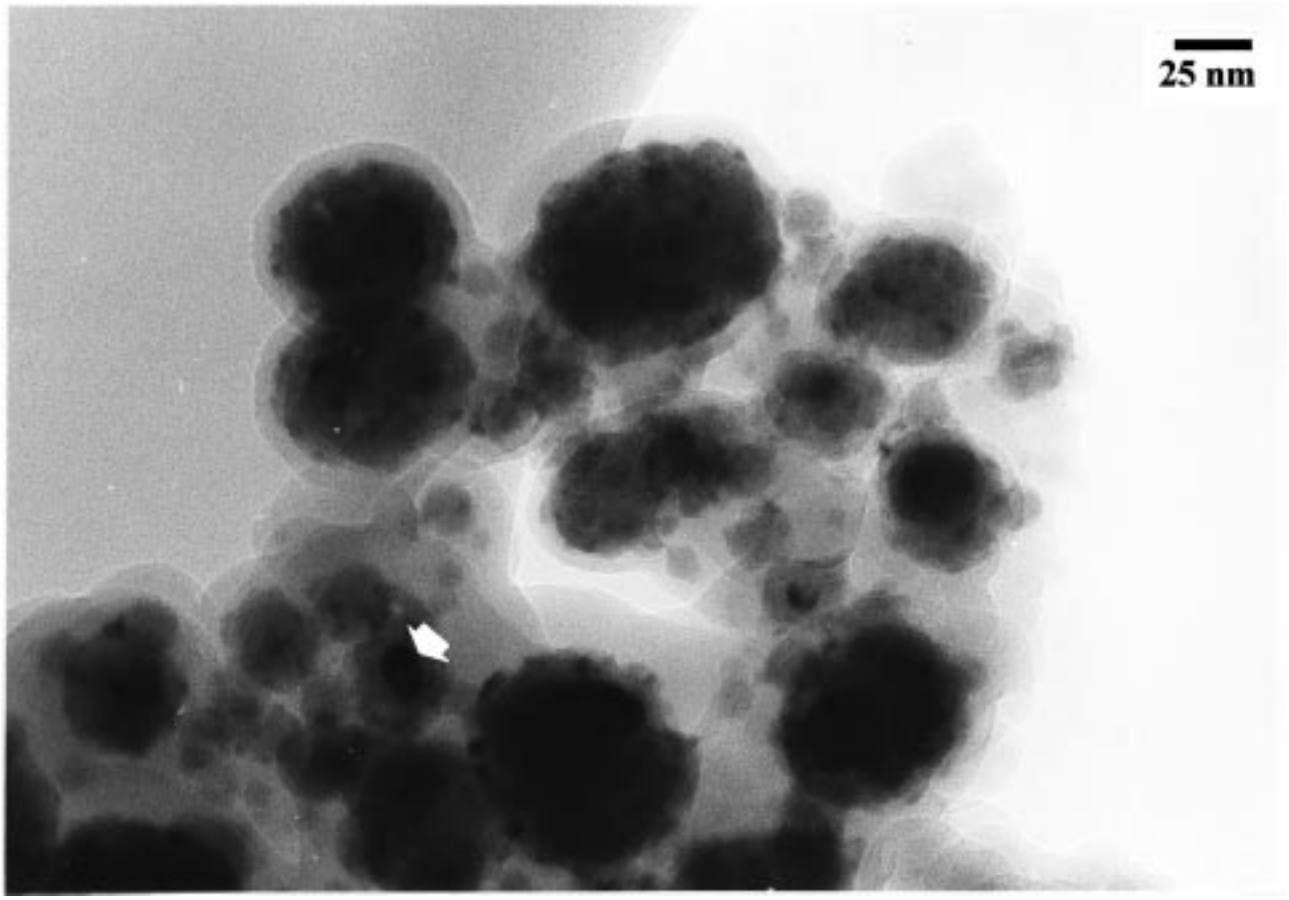

Figure 12. Transmission electron micrograph of the $NiSn/SiO_2$ sample after O_2 treatment at 673 K.

Table 8. Binding Energies (eV) of Core Electrons and XPS Atomic Ratios for $NiSn/SiO_2$ Catalyst after Different Treatment Conditions[a]

treatment	O 1s	Ni $2p_{3/2}$[b]	Sn $3d_{5/2}$[b]	Ni/Si	Sn/Si	Ni/Sn
H_2, 673 K	533.0	852.5 854.6	484.2 (38) 486.2 (31) 487.5 (31)	0.0200	0.0071	2.81
O_2, 673 K	533.0	852.8 854.4	484.1 (31) 486.0 (24) 487.2 (45)	0.0162	0.0059	2.74

[a] A value of 103.4 eV was obtained for the Si 2p peak in all experiments. [b] Values in parentheses indicate the relative percentage of surface species for each sample.

this may seem surprising, it is known that alloyed Sn with Pt shows greater resistance toward oxidation than metallic Sn.[15] In fact, surface characterization studies of PtSn and Pt_3Sn alloys have shown that surface compositions are readily altered by ion sputtering, annealing in a vacuum, or exposure to oxygen or hydrogen. For Pt_3Sn alloy, even the formation of a layer of tin oxide after air exposure has been proposed.[16]

On the other hand, the behavior of $PdSn/SiO_2$ was not far from that of $PtSn/SiO_2$ catalyst. After the reduction process the presence of palladium−tin alloys in the catalyst have been shown. The activation process with O_2 at 673 K resulted in the transformation of the alloys into phases richer in the noble metal, simultaneously with the segregation of tin oxide phases, as determined by XRD and TEM experiments. A part of surface tin remains as alloyed tin as was shown by XPS analysis, which confirms the presence of surface palladium−tin alloys after the oxidizing treatment.

From characterization and catalytic activity results, it appears that the silica-supported PtSn or PdSn alloys are inactive for CO oxidation reaction at low temperature. However, an oxidizing pretreatment of samples produced Pt_3Sn or Pd_3Sn_2 alloys and SnO_x phases. These new materials showed a good catalytic performance in the CO oxidation reaction. In fact, differences between chemisorption properties of Pt_3Sn and PtSn alloys have been established. Pt_3Sn chemisorbs oxygen more readily at lower temperature than PtSn,[17] and it has been admitted that oxygen chemisorbed on platinum plays an important role in the CO oxidation process over Pt/SnO_2 catalysts.[3] This interaction of O_2 with the alloys differs from its interaction with Pt or Sn separately.[18] However, the simultaneous formation of SnO_x phases is also an important feature. It must be taken into account that for both $PdSn/SiO_2$ and $PtSn/SiO_2$ catalysts XPS analysis showed a high enrichment of surface region on tin after O_2 or CO/O_2 treatments. The intimate contact between the metallic phase and SnO_x interface may be responsible for the enhanced activity showed by these systems as has been already proposed.[19] Actually we have shown that the oxidation of

(15) Cheung, T. T. P. *Surf. Sci.* **1986**, *177*, L887.
(16) Gardner, S. D.; Hoflund, G. B.; Schryer, D. R. *J. Catal.* **1989**, *119*, 179.
(17) Bouwman, R.; Toneman, L. H.; Holscher, A. *A. Surface Sci.* **1973**, *35*, 8.
(18) Hoflund, G. B.; Asbury, D. A.; Kirszenstejn, P.; Laitinen, H. A. *Surf. Sci.* **1985**, *161*, L583.
(19) Logan, A. D.; Paffett, M. T. *J. Catal.* **1992**, *133*, 179.

$PtSn/SiO_2$ and $PdSn/SiO_2$ materials at 673 K leads to the formation of silica-supported $Pt_xSn-SnO_2$ or $Pd_x-Sn-SnO_2$ systems, which may be related to some literature examples of Pt or Pd supported on SnO_2 which are low-temperature catalysts for the CO oxidation reaction.[2,10,11]

On the other hand, the performance of $NiSn/SiO_2$ in the CO oxidation reaction is similar to the Sn/SiO_2 sample.

It is concluded that the silica-supported Pt−Sn and Pd−Sn catalysts reported in this study could be useful materials in the CO oxidation reaction under CO_2 atmospheres at low temperatures.

Acknowledgment. We thank CICYT (MAT96-0859-C02) for financial support and the Serveis Cientifico-Tècnics UB for chemical analysis and apparatus facilities. We are also grateful to Prof. X. Solans (UB) for helpful discussions.

CM970728N